Journal of Sea Research 74 (2012) 8–15

Contents lists available at SciVerse ScienceDirect

Journal of Sea Research

journal homepage: www.elsevier.com/locate/seares

The ocean's internal motion: A short overview of NIOZ thermistor string observations

Hans van Haren

NIOZ Royal Netherlands Institute for Sea Research, P.O. Box 59, 1790 AB Den Burg, The Netherlands

ARTICLE INFO

Article history:
Received 5 September 2011
Received in revised form 29 March 2012
Accepted 27 April 2012
Available online 9 May 2012

Keywords:
Thermistor String Observations
Internal Wave–Turbulence
0.1–100 m vertical scales, 10–10000 s time-scales

ABSTRACT

Detailed observations of the variability in space and time of motions that dominate redistribution of material and heat are rare. However, these motions are vital for life in seas and ocean. Modern electronics have allowed the manufacturing of 1-Hz high-sampling rate, <1-mK precision, 6000-m depth-rated temperature sensors with the potential of 1-year uninterrupted stand-alone operation. These sensors have been specifically developed for use in a vertical array of many O(100), to study dynamic processes like fronts and internal waves in shallow seas and deep ocean. Under conditions of sufficient spatial vertical resolution, O(0.1–1 m), and temperature acting as a proper tracer for density variations, the sensors are excellent in estimating turbulence parameters generated by such processes. In the ocean interior, they reveal continuous internal wave variability and step-like vertical layering in temperature, but very little turbulence. Above sloping topography, small- and large-scale overturnings yield turbulence parameter values which vary by up to four orders of magnitude as a function of time. Largest values are observed in bursts lasting typically 500–1000 s and associated with nonlinear internal wave passages. These bursts occur irregularly in a tidal phase. When extrapolated to the ocean at large, sufficient mixing is observed above sloping boundaries to maintain the overall vertical density stratification.

1. Introduction

The surface of the Earth consists of 70% water, of which nearly 60% is in the southern hemisphere. The vertical range of ocean bottom topography is 20% larger than that of land. There are thus good reasons to study the dynamics of the largely unknown, globally important ocean interior, but not without losing sight of its geographical context. Sharp focus is needed when interpreting observations on ocean dynamics. At the start of my career I was taught to look carefully at graphs and figures by my promotor Jef Zimmerman. This paper combines in a short overview the development of detailed observations, mainly using moored temperature sensors, of variable ocean interior motions and the interpretation of their potential impact on the redistribution of material on small scales and on a global scale.

1.1. The Sun, the Moon, Earth's rotation and topography

Waves supported by the vertical density or momentum stratification in seas and ocean, 'internal waves' (IW), are generally found between inertial frequency f and buoyancy frequency N. They play an important role in the balance of stratification supporting energetic internal waves that produce vertical shear of horizontal currents which, in theory, should destroy the stratification. They are ubiquitous around the globe in estuaries, seas and oceans. Part of the context is extra-terrestrial, as Sun and Moon govern the main internal wave dynamics via tide generation, in association with the Earth's rotation, its spherical shape and topography.

The ocean, despite being stably stratified in density from surface to bottom mainly by solar insolation, also supports substantial turbulent mixing. Besides the influence of winds, this mixing is thought to be predominantly induced by internal wave breaking (Munk and Wunsch, 1998; Thorpe, 1987a), a partial sink for tidal energy. Since internal tides are generated via the interaction of horizontal motions with sloping underwater topography, it is conjectured that most mixing also occurs above topography rather than in the interior (Armi, 1978; Garrett, 1990, 1991; Munk, 1966; Thorpe, 1987b). If such mixing is efficient enough, it may suffice to represent the basin-wide vertical turbulent diffusivity, presently rated at $10^{-4}\,m^2\,s^{-1}$, needed to maintain the vertical density stratification in the ocean interior (Munk and Wunsch, 1998). At present and as previously suggested by Gregg (1989), there is no other candidate than ubiquitous internal waves to supply vertical turbulent diffusion at this rate.

The universality of internal wave spectra suggests that they are shaped by a saturation process (Munk, 1981). The vertical density stratification is thus found in a marginally stable state in terms of the gradient Richardson number: large stratification supports the largest internal wave shear to the point of [just] becoming unstable. This has been observed in the seasonally stratified North Sea (van Haren et al., 1999). In a marginal stable state the inferred vertical turbulent 'diapycnal' exchange across the stratification is not very large but

E-mail address: hans.van.haren@nioz.nl.

1385-1101/$ – see front matter © 2012 Elsevier B.V. All rights reserved.
doi:10.1016/j.seares.2012.04.008

still O(100) times larger than molecular diffusion. This turbulence rate does not destroy stratification, but provides sufficient exchange to supply nutrients from the bottom to the photic zone in a shelf sea.

The low-frequency near-inertial internal wave motions carry most of the turbulence-generating shear, because their vertical length-scale is relatively small (van Haren et al., 1999). As these motions are nearly purely horizontal and circular their shear-magnitude varies at much larger time-scales than the inertial period (van Haren, 2000). Large-scale stratification varies at the same, 'sub-inertial' time scales. Near-inertial motions are generated following geostrophic adjustment of disturbances like atmospheric storm passages (Gill, 1982) and fronts (Davies and Xing, 2005). They are an important internal wave source when they propagate freely from their sources as near-inertial waves (Gill, 1982). They are only dominated by semidiurnal tidal motions as internal wave source, except for limited areas like most of the Mediterranean and Baltic seas. Barotropic, surface gradient driven, tidal motions are forced by topography to convert about 20% of their energy to baroclinic, density gradient driven, internal tides (Munk and Wunsch, 1998). While barotropic tides have highly deterministic amplitude and phase resulting in a narrow spectral energy peak, baroclinic tides appear as relatively broadband (width ~10% of their central frequency). In a time series, amplitude and phase are ill-defined as these vary intermittently in groups of about 10 waves of limited O(100 m) vertical coherency extent. This intermittency is universal (Wunsch, 1975), for internal waves in general, and it is related to larger-scale variations in the supporting stratification.

The high-frequency "small-scale" internal waves near N are the natural motions following disturbance of stratification (Groen, 1948). These waves have relatively large vertical scale relative to that of near-inertial waves and they mostly propagate as interfacial waves along a pycnocline (e.g., Fig. 1). In frequency, they border turbulence (D'Asaro and Lien, 2000; van Haren, 2011), but it is unclear how energy transfers from internal wave source to turbulence dissipation. A possibility is via interaction with near-inertial shear. As linear, sinusoidal waves do not create turbulent diffusive mixing, it seems they should develop as non-linear waves prior to breaking and irreversible turbulence generation. So far, high-frequency nonlinear waves have been observed in groups of 4–10 waves, more or less in a rank-ordered fashion of largest wave first as is typical for a group of "solitary" waves (see, e.g., review by Helfrich and Melville, 2006). The similar intermittent occurrence of such high-frequency internal waves as that of low-frequency internal tides suggests a common medium in the form of stratification and variations therein, with an undetermined continuum in between. It has been suggested that energy cascades from the source, near-inertial and tidal motions, via the internal wave continuum to high-frequency waves provide an explanation, see Gregg (1989) for a review.

The typical mean interior turbulent eddy diffusivity of the stratified sea and upper ocean are estimated to be $K_z = 3 \pm 2 \times 10^{-5}$ m^2 s^{-1} (Gregg, 1989; van Haren et al., 1999). As mentioned above, such mean K_z are sufficient to explain the flux of nutrients into the photic zone and also the near-bottom temperature increase in the North Sea. It is suggested that this amount of turbulence is typical for a saturated internal wave field allowing for sparsely distributed turbulence, similar to surface wave white capping (Munk, 1981).

Here, an overview is presented of detailed observations demonstrating that internal wave motions above sloping topography are quite different from those in the ocean interior: they are not smoothly varying sinusoidal, but irregularly varying. High-resolution moored temperature sensors are the easiest means to facilitate process studies on internal wave-turbulence dynamics, provided they are used in areas where temperature has a known relationship with density variations. The sensors are also used to quantify several turbulence parameters, which are established using shipborne CTD and microstructure profiler. As such, a thermistor string has an advantage over the use of acoustic (backscatter) devices, which have provided more detailed images of internal wave–turbulence in the (recent) past (e.g., Moum et al., 2008; Pinkel, 1981), but which cannot quantify turbulence parameters such as eddy diffusivity. High resolution thermistor string thus provides additional information to eddy viscosity and turbulence dissipation rate estimates using acoustic Doppler current profiler (e.g., Lohrmann et al., 1990).

In Section 2, some of the technical details of ocean temperature observations are given. In Section 3, it will be explained how such observations can be used to estimate turbulence parameters. In Section 4, detailed moored temperature observations and turbulence estimates are presented from diverse sites in shallow seas and deep ocean. In Section 5, the contribution of internal wave breaking to general ocean mixing is discussed, before suggesting improvement for future instrumentation.

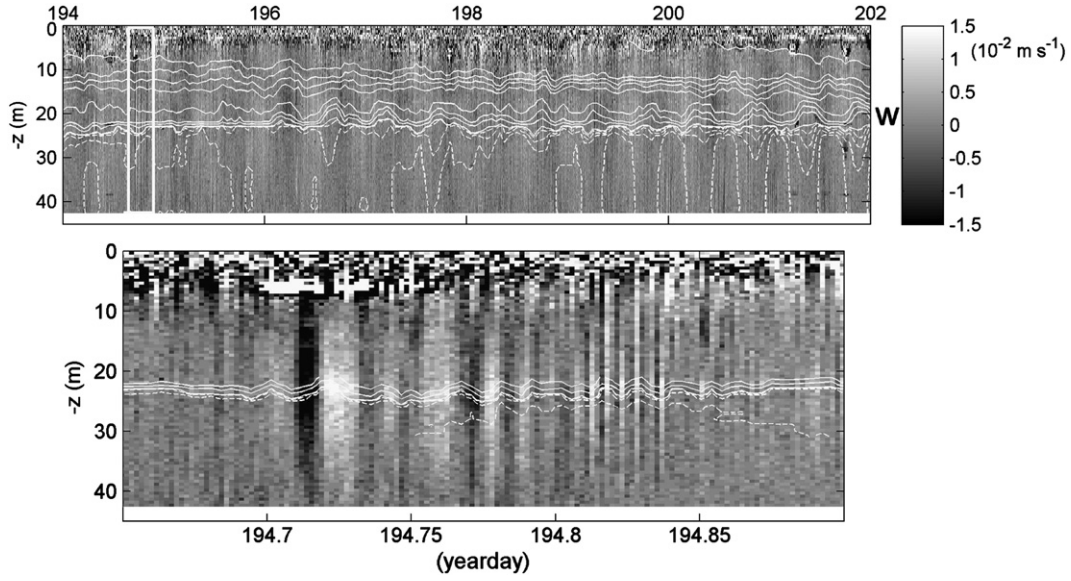

Fig. 1. Historic 1994 summertime central North Sea hourly smoothed temperature contours (white, every 1 °C between 10 and 18 °C (solid) and every 0.2 °C between 9.1 and 9.9 °C (dashed)) from 3 combined Aanderaa thermistor strings totalling 32 thermistors at 1 or 2 m vertical distance. Grey shading indicates vertical current (w) observed using a bottom-mounted, upward-looking 600 kHz acoustic Doppler current profiler (ADCP). The white box indicates the detailed lower panel, which includes only fast-sampled (once per 120 s) temperature contours of the lower pycnocline. The dark or spickled band between 0 and about −7 m represents bad (surface reflection side-band) ADCP-data.

2. Ocean temperature observations

To monitor the transition between internal wave sources and their turbulent sinks, that is non-linear internal waves and breaking, one has to resolve timescales down to O(1 s) and vertical scales O(0.1–1 m), much shorter than the buoyancy scales O(100–1000 s) and O(100 m). This excludes the smallest turbulence dissipation scales O(10^{-2} m), O(10^{-2} s), but is adequate to resolve the energetic turbulent overturning scales and all of the internal wave scales, provided measurements are done over ranges of at least a day in time and O(100 m) vertically and O(1000 m) horizontally. Presently, the measurement of horizontal scales is still a thought for future development.

Previously, such short turbulence/internal wave scales have been resolved using accurate temperature sensors near the surface, but mainly as a single vertical string towed behind and powered by a ship (e.g., Marmorino, 1987) or from a device that floats freely for a period of a few days (Cairns, 1975). Near the ocean bottom at great depths few 1-mK accurate stand-alone instruments have resolved the above scales over short periods of a day (Thorpe, 1987b) up to two weeks (van Haren et al., 2005). Historic off-the-shelf moorable thermistor strings suffered from inadequate resolution (>20 mK), memory capacity (<1 week data sampled at a rate of once per 30 s or longer) and thermal response time (>100 s). In Fig. 1 an example is given of such historic data, which, nevertheless, just resolve the small internal wave but not the large-turbulence scales. At NIOZ, this initiated development of more accurate, low-energy consuming temperature sensors.

The recently designed 'NIOZ3' stand-alone thermistor is versatile and can be used attached to various mooring devices like bottom landers and taut mooring cables at slopes as well as in the open ocean down to 6000 m, having 0.25 s response time and sampling with a precision better than 1 mK and noise level of 40 μK at a rate of 1 Hz for the period of a year (van Haren et al., 2009). The sensors are attached to a nylon-coated steel cable or a lander using Japanese electricians tape (generally in the color yellow). This tape has a superb characteristic in sea water and it allows flexible distances between sensors. When two or more sensors are mounted on a conductive cable they are synchronized to a single standard clock via induction. In principle, a large amount of sensors can thus be reached at arbitrary mutual distances, tested up to at least 500 m cable length away from the "synchronizer" and up to 0.5 m from the cable. The same method of induction is used to communicate with the sensors, of which 110 have been built. Of its smaller successor 'NIOZ4', an upgrade which has similar characteristics, 200 have been built so far.

These NIOZ-T sensors are designed to specifically study internal waves and the energetic turbulent overturning motions that may contribute to mixing and redistribution of material in the ocean. The strength of the total design lies in the use of O(100) sensors in a single string, whereby rapid relative temperature variations are adequately resolved in time and vertical dimension, adapted for each area of investigation. Regular calibration to 0.001 °C accuracy is performed in situ using CTD held still in near-homogeneous, internal wave generated layers, and before and after deployment at sea in a custom-made laboratory calibration bath. During post-processing, non-aged sensor drift (varying between 10^{-4} and 10^{-3} °C/week) is corrected to within a precision of <0.001 °C by comparing weekly mean values. Profiles of these mean temperatures cannot be affected by turbulent overturns and are to be statically stable. Recently, new sensors are pre-aged before manufacturing, to reduce the drift by at least a factor of 10.

3. Turbulence parameter estimates

One can estimate turbulence parameters like dissipation rate ε and vertical eddy diffusivity K_z using vertically densely sampled variations in density, as proposed by Thorpe (1977). This has been done using shipborne free falling microstructure profiler and CTD, but seldom using moored instrumentation. Few adequate and affordable moorable CT-sensors exist. Although both salinity and temperature contribute to density variations, there are (parts of) seas and oceans where they contribute spatially and temporally consistent way. An example is the upper 1000 m of the NE Atlantic Ocean around mid-latitudes, well above the Mediterranean outflow waters. In such areas where temperature can be effectively used as tracer for density variations and temperature sensors can be used to estimate turbulence parameters. For such estimates we require a tight, unambiguous across the thermistor range and time independent, and preferably linear relationship between temperature and density. Such relationship is verified and established via CTD observations in the vicinity of a thermistor mooring. Thus, turbulence parameters are estimated over the vertical array of densely spaced NIOZ thermistor-data every 1 s as follows.

Turbulent overturning is estimated from displacements (d) in rearranging (sorting) an observed potential density (temperature) profile into a stable monotonic profile without inversions (Thorpe, 1977). In order to relate displacements to turbulence, they are compared with the largest turbulent overturning scale in stratified flows, the Ozmidov scale $L_O = \varepsilon^{1/2} N^{-3/2} = 0.8d$ (Dillon, 1982; Thorpe, 1977). The numerical constant value is empirically determined (Dillon, 1982) and N(z,t) is computed from the reordered profile. Originally, the rms-value of d averaged over the largest overturn was used, but in practice overturns are difficult to define in a turbulent environment with a variety of scales and they regularly exceed the range of thermistors. Therefore, we use complete profiles of d(z) in the computation of turbulence parameter estimates. This gives depth-time series,

$$\varepsilon(z,t) = 0.64 d^2 N^3, \quad (1)$$

and, using the relation $K_z = \Gamma \varepsilon N^{-2}$ (Osborn, 1980) with a constant mixing efficiency $\Gamma = 0.2$ for the conversion of kinetic into potential energy,

$$K_z(z,t) = 0.128 d^2 N. \quad (2)$$

Subsequently, these parameters can be averaged over suitable vertical and time scales. Some tests with different ways of averaging are described in van Haren and Gostiaux (2012). The tests resulted in only small differences between the direct averaging of eddy diffusivity in comparison with the more appropriate averaging of the vertical heat flux first prior to calculation of the mean eddy diffusivity.

4. Observations

4.1. The ocean interior

Oscillatory tidal and high-frequency internal wave motions appear as smooth, linear waves in the summer-stratified central North Sea (Fig. 1). These motions resemble much better resolved open ocean motions that will be presented below and which have provoked similar vertical turbulent exchange characteristics that were established using CTD, as indicated in Section 1.

The stratified shallow seas and open ocean interior are in fact permanently in motion, with typical ocean amplitudes reaching several tens of meters, as appears from Fig. 2, which shows a two-day example composite of 53 NIOZ thermistor sensors sampling stratification around 1400 m in the Canary Basin, NE Atlantic Ocean. The weakly turbulent motions are smooth, not perfectly sinusoidal in shape, and have relatively large vertical coherent scales with near-zero phase difference over the range of thermistors ("local vertical mode-1"), at both tidal and near-buoyancy frequencies. This local mode-1 appearance is found throughout the 1.5 year record, but amplitudes vary continuously for motions having frequencies within any particular finite frequency band. Over the 130 m sensor range, the stratification is also subject to substantial variation. Thickness of strongly stratified

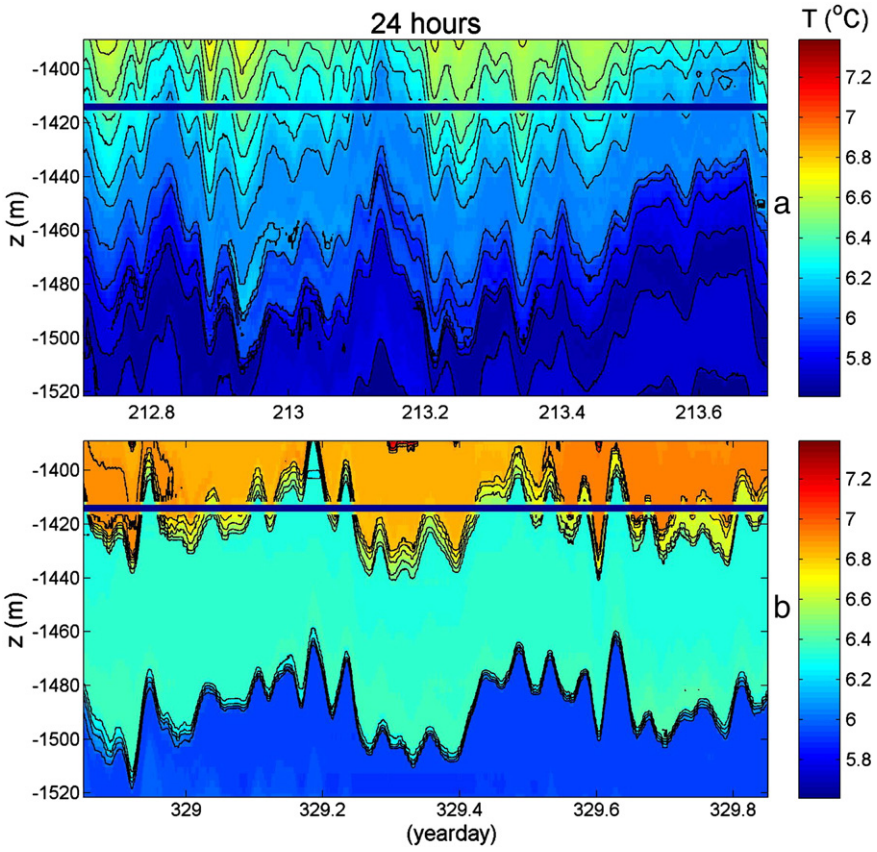

Fig. 2. Open ocean internal wave motions observed using 54 NIOZ3 sensors at 2.5 m vertical intervals sampling at a rate of 1 Hz in 2006. The thermistor string was directly below the top-buoy of a 3800 m long mooring in the Canary Basin NE Atlantic Ocean. The horizontal line indicates a failing sensor. In black, isotherms every 0.1 °C. Two arbitrary 24 hour time-span examples are given in panels a and b. Layering thickness is varying strongly with time, some influence of Mediterranean salinity is visible in the apparent temperature inversion layers: e.g., in a. below 1450 m and especially between days 212.8 and 213.2, in b. in the ranges [1410, 1420] m and [1460, 1480] m.

layers drops below sensor separation, in this case 2.5 m (Fig. 2b; e.g., 6.2 and 6.6 °C isotherms), while weakly stratified layers can exceed half the sensor range (Fig. 2b; between 1420 and 1480 m). Overturns are few and far apart, despite the 1-Hz sampling. However, due to the ill-defined density-temperature relation, which varies in time and space with these varying water masses under intermediate Mediterranean Sea influence, quantification of turbulence parameters is difficult. In addition, a small range of the larger overturn scales is resolved by the 2.5 m vertical sensor separation, as the mean Ozmidov scale $<L_O> \approx 0.4$ m (obtained from high-resolution shipborne CTD-data). Instead, turbulence parameter estimates are made using limited conventional CTD-observations at stations nearby which provide typical values of $K_z = 2\text{–}3 \times 10^{-5}$ m^2 s^{-1} and $\varepsilon \approx 10^{-9}$ W kg^{-1} over the range of the thermistors. These values are in the same range as previously estimated from upper (<2000 m) open ocean microstructure observations (e.g., Gregg, 1989).

4.2. A frontal change of tidal phase

Quite different and much more turbulent are internal wave motions near sloping topography. Although bottom slopes are on average just a few per cent and typical internal tide generating horizontal currents are 0.1 m s^{-1}, the impact of such currents and slopes is spectacular in their production of wave breaking in the near-interior. Turbulent overturning ranges from 10 to 50 m vertical scales (Fig. 3) and it dominates sediment resuspension involving local vertical currents O(0.1) m s^{-1} (Hosegood et al., 2004).

Applying Eqs. (1) and (2) to thermistor data around the sudden change from warming to cooling tidal phase associated with an upslope moving frontal bore, provides an image of large turbulent eddy diffusivities and associated turbulence dissipation rates (Fig. 3). The essentially 3-D part in the depth-time temperature plot is entirely due to turbulent overturns while the reordered stable stratification is characterized by very thin (down to the lowest vertical resolution, in this case $\Delta z = 0.5$ m, much smaller than $<L_O> \approx 20$ m) layering that approaches the bottom to within a meter just prior to a frontal passage (van Haren and Gostiaux, 2012).

Large displacements are observed at and just before the arrival of a 40–50 m high nonlinear front that occurs once or twice a tidal period. Eddy diffusivity reaches $K_z = 10^{-1}\text{–}10^{0}$ m^2 s^{-1}, turbulent dissipation rate $\varepsilon = 10^{-5}\text{–}10^{-4}$ W kg^{-1}. The front itself is the only large overturn extending from the bottom upward, thus being important for sediment resuspension. The turbulent heat flux $K_z d\theta/dz$, θ denoting potential temperature, and dissipation rate are largest at the frontal bore, and relatively smaller in the weakly stratified large overturns preceding it where K_z is largest. These large interior overturns are associated with relatively large downward motions originating from above the thermistor string. This downdraught seems part of the turbulent bore moving up the slope. The front is sharpened when the interior overturns just preceding it are large and more intense. Behind the front the trailing near-N waves also turn-over, but in rapidly decreasing magnitude. Averaged over time, over a two-week spring-neap period, and over depth, over the range of thermistors being 50 m here, gives $<\varepsilon> = 1.5 \pm 0.7 \times 10^{-7}$ W kg^{-1}, $<K_z> = 3 \pm 1 \times 10^{-3}$ m^2 s^{-1}. These mean 'sloping topography' values are 100-times observed open ocean values.

4.3. Small-scale overturning

Above sloping topography not only large overturns are observed due to a frontal bore, but also quasi-permanently bursts of smaller

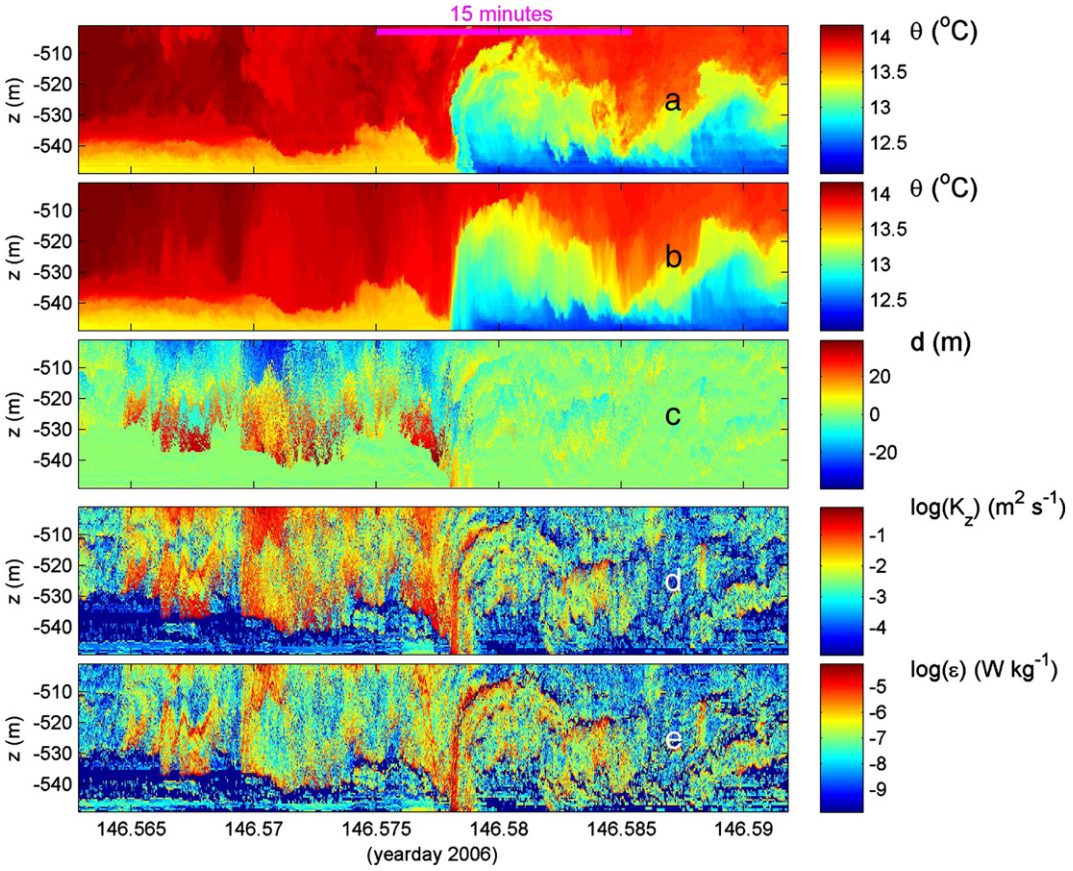

Fig. 3. Depth-time series of temperature and computed variables during 2500 s prior to and into an upslope, cooling tidal phase: a frontal passage and associated peaks in turbulent mixing with large overturns, sampled at a rate of 1 Hz at 0.5 m vertical intervals between 0.5 and 50 m above a slope of Great Meteor Seamount (NE Atlantic Ocean). The three gaps in the data due to missing thermistors (out of 101) have been filled by linearly interpolation using data from their neighbours. a. Potential temperature (θ) data, after pressure-corrected calibration. b. Re-ordered potential temperature profiles every 1-Hz time-step. c. Displacements following comparison of a. and b. d. Eddy diffusivity computed using Eq. (2) and a potential density(ρ)–potential temperature relationship of $\delta\rho/\delta\theta = -0.101$ kg m^{-3} °C^{-1} for all of the individual displacements in c. e. Turbulence dissipation rate, estimated using Eq. (1). In d. and e. dark-blue also indicates below threshold.

overturns are found throughout a tidal period (Fig. 4). For example, during the warming tidal phase, turbulence mainly occurs in the stratified waters well away from the bottom in patches of typically 1–10 m thickness and of 30–300 s duration. They are part of high-frequency overturning Kelvin–Helmholtz shear instabilities (van Haren and Gostiaux, 2010). These instabilities are indirectly associated with the large-scale inertial-tidal shear, and with the smaller near-N internal waves that often appear in a local vertical mode-2 fashion with apparent vertical π-phase difference between isotherms rather than mode-1 (vertical 0 phase difference between isotherms) that was found almost exclusively in the open ocean observations. In the O(1–10 m) high turbulence patches away from the bottom, turbulence parameter values are $K_z = 10^{-3}$–10^{-1} m^2 s^{-1}, $\varepsilon = 10^{-6}$–10^{-5} W kg^{-1}. The average $<L_O> \approx 1.8$ m and some patches are short-lived O(10^1–10^2 s). Of these patches, those generated by Kelvin–Helmholtz instabilities contribute substantially to vertical exchange (Fig. 4e).

4.4. The shallow sea

What is observed above a large guyot in the deep ocean has been observed above many different sloping bottoms (e.g., Bonnin et al., 2006; Hosegood et al., 2004; Klymak and Moum, 2003). These are not all presented here, except for a few outliers. Such include internal wave breaking in a [very] shallow sea: near a beach under calm weather conditions (Fig. 5). The location was near Texel beach pole 13, The Netherlands (van Haren et al., 2012). There, having similar time scales but obviously different vertical scales, fronts (Fig. 5a, day 180.33), small-scale internal waves (e.g., days 180.28, 180.31) and turbulent displacements (Fig. 5b) are all observed using NIOZ4 sensors at $\Delta z = 0.042$ m $<< L_O > \approx 0.15$ m, sampled at 2 Hz. These observations are made in shallow water well offshore the surf zone, when surface (wind) waves have heights <0.1 m, in the middle between two breakwaters. Wind speeds are <0.2 m s^{-1} and the water is warmed by solar radiation from day 180.26 onward.

Due to the smaller vertical range O(1 m) and buoyancy period O(100 s) than those of the open ocean observations above, turbulence parameters are on average 10–100 times smaller: throughout the depth-time range of observations $K_z \approx 10^{-5}$ m^2 s^{-1} (and $\varepsilon \approx 10^{-8}$ W kg^{-1}; not shown). These values are associated with short-period weak overturning. Internal wave amplitudes, stratification and internal wave-induced turbulence gradually intensify around time of high-water. Highest values ($K_z = 10^{-3}$ m^2 s^{-1}; $\varepsilon = 10^{-5}$ W kg^{-1}) are in the upper half of the observational depth-range. Although the tide directly influences these internal motions by having a 1.5 m vertical range, internal wave mixing seems to be mainly driven by the atmosphere and small-scale internal waves (van Haren et al., 2012). Averaged over the 10 h and entire vertical range of observations, eddy diffusivity is similar to open ocean values: $<K_z> = 2 \times 10^{-5}$ m^2 s^{-1}, whereas $<\varepsilon> = 6 \times 10^{-8}$ W kg^{-1}, $<N> = 3 \times 10^{-2}$ s^{-1}.

4.5. The deep non-tidal sea

Being relatively weak, it appears unlikely that tides govern internal wave turbulence in seas like [most of] the Mediterranean and the

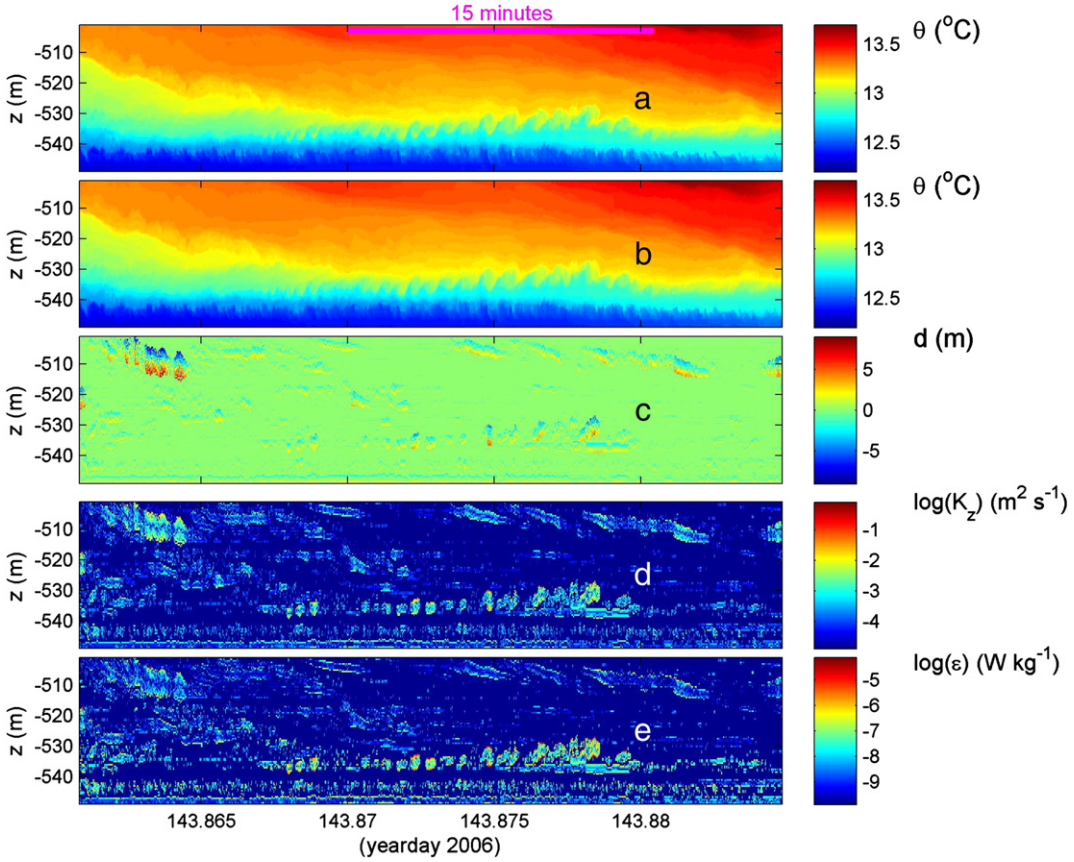

Fig. 4. As Fig. 3, but for a 2000 s example during a warming tidal phase. Scales have been modified for panels a.–c.

Baltic. There, the dominant low-frequency internal waves are near-inertial waves. In the deep Mediterranean around 4000 m, a one-year record of 103 NIOZ4 thermistors at intervals $\Delta z = 1.0$ m, much smaller than $<L_O> \approx 45$ m demonstrates a highly dynamic environment with a dominant inertial period and turbulent overturning (van Haren and Gostiaux, 2011). However, variations in temperature

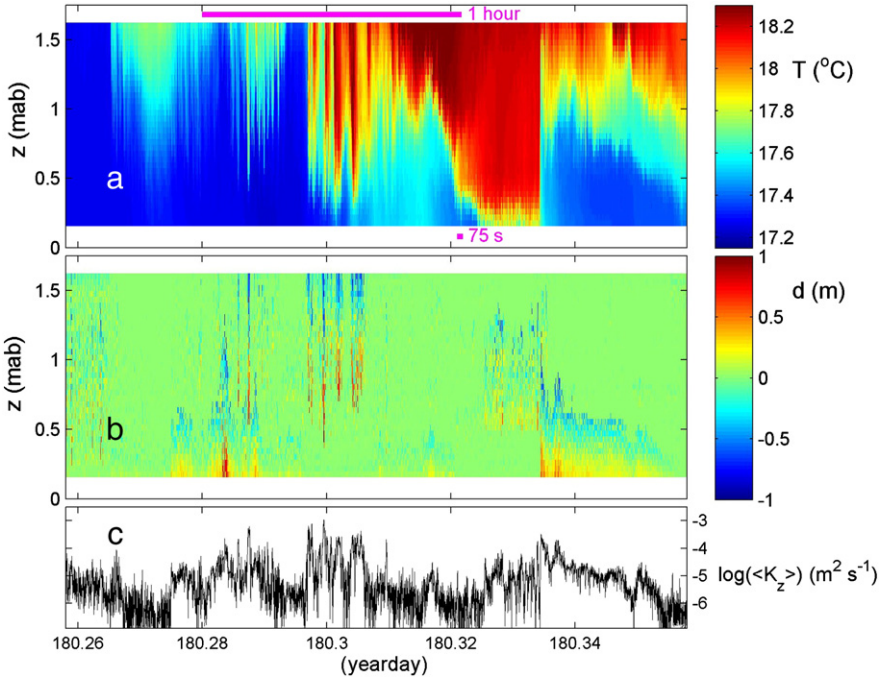

Fig. 5. Very shallow water internal wave–turbulence, observed near beach pole 13 at the Dutch island of Texel in mid-summer 2010. Depth-time series of 2-Hz sampled temperature and computed turbulence parameters during 8000 s around high-water, observed using 36 NIOZ4 sensors placed 0.042 m apart on a wooden pole. a. Observed 1-Hz T-data. b. Overturning displacements following comparison of a. with its reordered data. c. Time series of vertically averaged eddy diffusivity using Eq. (2) and $\delta\rho/\delta T = -0.23$ kg m^{-3} °C^{-1}.

are so weak, that analysis can only be made relative to the local adiabatic lapse rate $\Gamma = 1.86876 \times 10^{-4}$ °C m^{-1} of pressure effects on temperature so that stably stratified temperature can increase with depth.

A typical relative ΔT-image, $\Delta T = T - T_0 - \Gamma(z - z_0)$ where $T_0(z_0)$ denotes temperature at $z_0 = 4026$ m, has a range of ±0.0015 °C, within which all meso-, inertial- and small-scale variabilities occur (Fig. 6). Large-scale coherent motions exceed the entire 102-m range of thermistors, demonstrating small vertical phase shifts, best visible from comparison between the two isopycnals inferred from current meters. These phase shifts are indicative of vertical wave propagation. This is direct evidence of non-traditional inertial waves propagating in near-homogeneous waters ($N = 4.5 \times 10^{-5}$ s^{-1} = 0.53f), confirming earlier observations (van Haren and Millot, 2004, 2005) and theoretical work (e.g., Gerkema and Shrira, 2005; Gerkema et al., 2008 for a review). These waves have $O(1) = |w_f|/|\mathbf{u}_f|$ aspect ratio, and their vertical currents $|w_f| \leq 2.5 \times 10^{-2}$ m s^{-1} are relatively large, commensurate their vertical isotherm excursions typically exceeding 200 m (peak-trough).

In these data turbulence parameter analysis is seriously hampered by a lack of information on the salinity contribution to density variations. Only a crude estimate can be made computing Eqs. (1) and (2) based on ΔT-observations alone. This results in 1.5 days, vertically 100 m mean $\langle K_z \rangle = 10^{-2}$ m^2 s^{-1} and $\langle \varepsilon \rangle = 2 \times 10^{-10}$ W kg^{-1}. Thus, although turbulent heat fluxes are weak because of the weak density (temperature) stratification, and half an order of magnitude smaller than upper ocean values, turbulent overturns are large. The turbulent convection layers are mainly driven by near-inertial motions, suggesting a direct coupling between internal waves and turbulence.

5. Discussion and conclusions

Let us return from the small internal wave–turbulence scales in the ocean interior to their effects on the larger basin-wide scales.

Following Armi (1979) and Garrett's (1990) suggestion that roughly 10% of the ocean is occupied by bottom boundary layers above sloping topography, we compute an overall mean ocean-basin-interior $K_z \approx 3 \times 10^{-4}$ m^2 s^{-1}, a tenth of the mean K_z estimated from GMS-guyot NIOZ3 thermistor data and from microstructure profiler data over the Hawaiian Ridge (Aucan et al., 2006; Klymak et al., 2006). Such basin-wide eddy diffusivity value would be sufficient to explain the ocean's interior heat budget with a vertical advection–diffusion balance to maintain the density stratification in the ocean (Munk and Wunsch, 1998). This supports earlier conjectures (e.g., Armi, 1978; Garrett, 1990; Munk, 1966) for the importance of sloping boundary mixing.

Previous and present data suggest that such mixing is quite universal and independent of slope or forcing mechanism/frequency. Tides are not the only forcing mechanism, as turbulent overturns are also observed in seas where tides are weak. Bottom slopes need not be "critical": they do not need to match the angle of an internal wave ray for a wave of particular frequency, as vigorous bore-like motions have been observed at a variety of [tidally] non-critical slopes (e.g., Bonnin et al., 2006; Hosegood et al., 2004; Klymak and Moum, 2003). Near-inertial shear, the largest internal wave shear outside internal tidal generation areas, is important for (high-frequency) internal wave breaking in the interior, in case shear-induced mixing is the dominant turbulence generation process. Thus, most internal wave–turbulence transition seems associated with (nonlinear) deformation of internal wave motions near (local) buoyancy frequencies.

Above sloping bottoms large turbulence activity is observed, which make such areas completely different from the open ocean. The ocean interior is a much smoother linear wave-like environment, but it, naturally too, is in permanent motion rather than quiescent. This ocean in permanent motion is driven by surprisingly weak energetic forcing (Munk and Wunsch, 1998). Of all the power of 50-m breaking waves above topography, while highly important for life and redistribution of sediment in the ocean, very little is sensed at the surface. Therefore, in order to learn more about internal wave–turbulence processes it is mandatory to continue studying their characteristics in the sea and ocean interiors.

Future instrumentation development should be directed to a truly four-dimensional, 3-D spatial plus temporal, resolution of the internal wave–turbulence motions to understand their intrinsic properties. This could be establishable via a multi-string mooring, or floatation

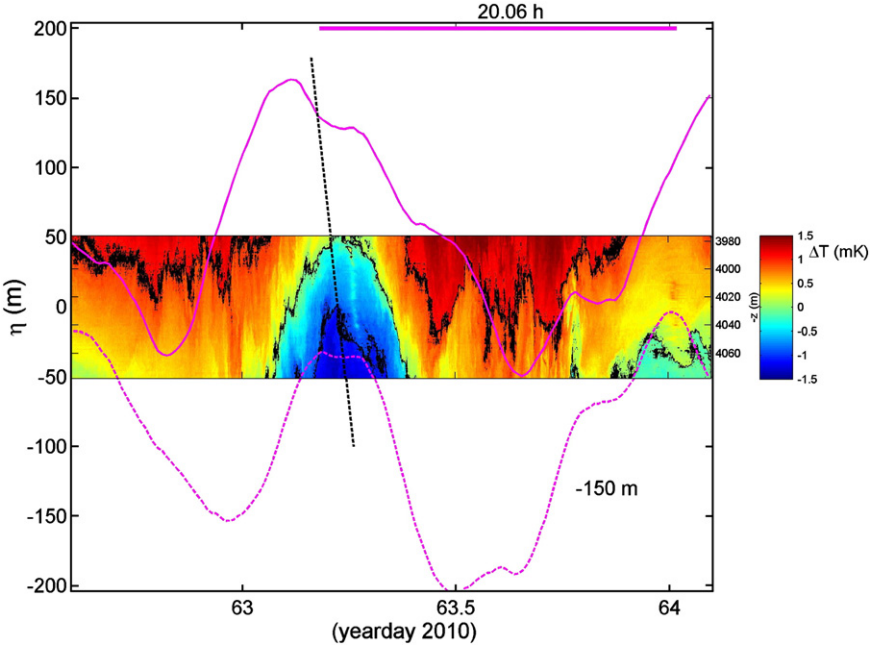

Fig. 6. Deep Mediterranean (Ionian Sea, near Greece) large internal wave–turbulence observations under extremely weakly stratified conditions. One-and-a-half day composite of vertical excursions computed using vertical current meter data (purple graphs) and 10-s smoothed T-observations relative to the adiabatic lapse rate (note the total temperature range of 3 mK). The upper current meter excursion is around its mean depth of 3975 m; that of the lower should be displaced 150 m deeper. The straight black dashed line indicates an approximate phase change. Largely, the computed excursions match those of the detailed T-observations, which are sampled at 1 Hz and 1 m vertical intervals. In black, relative isotherms are indicated every mK. Note that the contour lines are thin, but appear thick in places due to the numerous overturns. The local inertial period is 20.06 h.

device (Thorpe, 2010). Typical turn-over scales generated by Kelvin–Helmholtz instabilities and bores are O(1–10 m) which we want to resolve to study their evolution, whereas typical internal wave lengths are O(10^3 m). A small array would study internal wave–turbulence resolving the former spatial scales, and a large array the statistical properties and internal wave propagation.

Acknowledgments

I thank the crews of the R/V Pelagia and FS Meteor and NIOZ-MTM for deployment and recovery of moorings. I am greatly indebted to Martin Laan, Louis Gostiaux and Dirk-Jurjen Buijsman for the continuing pleasant cooperation during development of NIOZ-thermistors. Construction and deployment of NIOZ-thermistors were financed in part by investment grants ('Oceanographic equipment', 'LOCO', 'KM3NeT') from Netherlands Organization for the Advancement of Scientific Research, NWO and by BSIK. This paper benefited from the constructive comments of two anonymous reviewers and the handling editor.

References

Armi, L., 1978. Some evidence for boundary mixing in the deep ocean. Journal of Geophysical Research 83, 1971–1979.
Armi, L., 1979. Effects of variations in eddy diffusivity on property distributions in the oceans. Journal of Marine Research 37, 515–530.
Aucan, J., Merrifield, M.A., Luther, D.S., Flament, P., 2006. Tidal mixing events on the deep flanks of Kaena Ridge, Hawaii. Journal of Physical Oceanography 36, 1202–1219.
Bonnin, J., van Haren, H., Hosegood, P., Brummer, G.-J.A., 2006. Burst resuspension of seabed material at the foot of the continental slope in the Rockall Channel. Marine Geology 226, 167–184.
Cairns, J.L., 1975. Internal wave measurements from a mid-water float. Journal of Geophysical Research 80, 299–306.
D'Asaro, E.A., Lien, R.-C., 2000. The wave–turbulence transition for stratified flows. Journal of Physical Oceanography 30, 1669–1678.
Davies, A.M., Xing, J., 2005. The effect of a bottom shelf front upon the generation and propagation of near-inertial internal waves in the coastal ocean. Journal of Physical Oceanography 35, 976–990.
Dillon, T.M., 1982. Vertical overturns: a comparison of Thorpe and Ozmidov length scales. Journal of Geophysical Research 87, 9601–9613.
Garrett, C., 1990. The role of secondary circulation in boundary mixing. Journal of Geophysical Research 95, 3181–3188.
Garrett, C., 1991. Marginal mixing theories. Atmosphere–Ocean 29, 313–339.
Gerkema, T., Shrira, V.I., 2005. Near-inertial waves in the ocean: beyond the "traditional approximation". Journal of Fluid Mechanics 529, 195–219.
Gerkema, T., Zimmerman, J.T.F., Maas, L.R.M., van Haren, H., 2008. Geophysical and astrophysical fluid dynamics beyond the traditional approximation. Reviews of Geophysics 46, RG2004. http://dx.doi.org/10.1029/2006RG000220.
Gill, A.E., 1982. Atmosphere–ocean Dynamics. Academic Press, Orlando Fl, USA. 662 pp.
Gregg, M.C., 1989. Scaling turbulent dissipation in the thermocline. Journal of Geophysical Research 94, 9686–9698.
Groen, P., 1948. Contribution to the theory of internal waves. K.N.M.I. Med. Verh., B11, pp. 1–23.
Helfrich, K.R., Melville, W.K., 2006. Long nonlinear internal waves. The Annual Review of Fluid Mechanics 38, 395–425.
Hosegood, P., Bonnin, J., van Haren, H., 2004. Solibore-induced sediment resuspension in the Faeroe–Shetland Channel. Geophysical Research Letters 31, L09301. http://dx.doi.org/10.1029/2004GL019544.
Klymak, J.M., Moum, J.N., 2003. Internal solitary waves of elevation advancing on a shoaling shelf. Geophysical Research Letters 30, 2045. http://dx.doi.org/10.1029/2003GL017706.
Klymak, et al., 2006. An estimate of tidal energy lost to turbulence at the Hawaiian Ridge. Journal of Physical Oceanography 36, 1148–1164.
Lohrmann, A., Hackett, B., Røed, L.P., 1990. High resolution measurements of turbulence, velocity and stress using a pulse-to-pulse coherent sonar. Journal of Atmospheric and Oceanic Technology 7, 19–37.
Marmorino, G.O., 1987. Observations of small-scale mixing processes in the seasonal thermocline. Part II: wave breaking. Journal of Physical Oceanography 17, 1348–1355.
Moum, J.N., Nash, J.D., Klymak, J.D., 2008. Small-scale processes in the coastal ocean. Oceanography 21, 23–33.
Munk, W., 1966. Abyssal recipes. Deep Sea Research 13, 707–730.
Munk, W., 1981. Internal waves and small-scale processes. In: Warren, B.A., Wunsch, C. (Eds.), Evolution of physical oceanography. MIT Press, Cambridge MA, USA, pp. 264–291.
Munk, W., Wunsch, C., 1998. Abyssal recipes II: energetics of tidal and wind mixing. Deep-Sea Research I 45, 1977–2010.
Osborn, T.R., 1980. Estimates of the local rate of vertical diffusion from dissipation measurements. Journal of Physical Oceanography 10, 83–89.
Pinkel, R., 1981. Observations of the near-surface internal wave field. Journal of Physical Oceanography 11, 1248–1257.
Thorpe, S.A., 1977. Turbulence and mixing in a Scottish loch. Philosophical Transactions of the Royal Society of London. Series A: Mathematical and Physical Sciences 286, 125–181.
Thorpe, S.A., 1987a. Transitional phenomena and the development of turbulence in stratified fluids: a review. Journal of Geophysical Research 92, 5231–5248.
Thorpe, S.A., 1987b. Current and temperature variability on the continental slope. Philosophical Transactions of the Royal Society of London. Series A: Mathematical and Physical Sciences 323, 471–517.
Thorpe, S.A., 2010. Breaking internal waves and turbulent dissipation. Journal of Marine Research 68, 851–880.
van Haren, H., 2000. Properties of vertical current shear across stratification in the central North Sea. Journal of Marine Research 58, 465–491.
van Haren, H., 2011. Internal wave–turbulence pressure above sloping sea bottoms. Journal of Geophysical Research 116, C12004. http://dx.doi.org/10.1029/2011JC007085.
van Haren, H., Millot, C., 2004. Rectilinear and circular inertial motions in the Western Mediterranean Sea. Deep-Sea Research I 51, 1441–1455.
van Haren, H., Millot, C., 2005. Gyroscopic waves in the Mediterranean Sea. Geophysical Research Letters 32, L24614. http://dx.doi.org/10.1029/2005GL023915.
van Haren, H., Gostiaux, L., 2010. A deep-ocean Kelvin–Helmholtz billow train. Geophysical Research Letters 37, L03605. http://dx.doi.org/10.1029/2009GL041890.
van Haren, H., Gostiaux, L., 2011. Large internal waves advection in very weakly stratified deep Mediterranean waters. Geophysical Research Letters 38, L22603. http://dx.doi.org/10.1029/2011GL049707.
van Haren, H., Gostiaux, L., 2012. Detailed internal wave mixing observed above a deep-ocean slope. J Mar Res 70, 173–197.
van Haren, H., Maas, L., Zimmerman, J.T.F., Ridderinkhof, H., Malschaert, H., 1999. Strong inertial currents and marginal internal wave stability in the central North Sea. Geophysical Research Letters 26, 2993–2996.
van Haren, H., Groenewegen, R., Laan, M., Koster, B., 2005. High sampling rate thermistor string observations at the slope of Great Meteor Seamount. Ocean Science 1, 17–28.
van Haren, H., Laan, M., Buijsman, D.-J., Gostiaux, L., Smit, M.G., Keijzer, E., 2009. NIOZ3: independent temperature sensors sampling yearlong data at a rate of 1 Hz. IEEE Journal of Oceanic Engineering 34, 315–322.
van Haren, H., Gostiaux, L., Laan, M., van Haren, M., van Haren, E., Gerringa, L.J.A., 2012. Internal wave turbulence near a Texel beach. PLoS One 7 (3), e32535. http://dx.doi.org/10.1371/journal.pone.0032535.
Wunsch, C., 1975. Internal tides in the ocean. Reviews of Geophysics and Space Physics 13, 167–182.